# A New Image Compression by Gradient Haar Wavelet

** Yaser Sadra*


## Abstract

**With the development of human communications, the usage of visual communications has also increased. The advancement of image compression methods is one of the main reasons for the enhancement. This paper first presents main modes of image compression methods such as JPEG and JPEG2000 without mathematical details. Also, the paper describes gradient Haar wavelet transforms in order to construct a priliminary image compression algorithm so that sub images inherit the same amount of original image information. Then, a new image compression method is proposed based on the preliminary image compression algorithm that can improve standards of image compression. The new method is compared with original modes of JPEG and JPEG2000 (based on Haar wavelet) by image quality measures such as MAE, PSNAR, and SSIM. The image quality and statistical results confirm that can boost image compression standards. It is suggested that the new method is used in a part or all of an image compression standard.**


***Keywords :*** **Digital images, image communication, image decomposition, image storage, image quality, wavelet transforms**

## I. INTRODUCTION

Nowadays, digital images and videos play a significant role in human communications [1-6]. With the advancement of sciences such as social networks, telecommunication, and deep space communication, the amount of data that needs to be transferred increases, therefore, it causes slow communication and expensive storage [7-10]. In the field of deep space communication, The National Aeronautics and Space Administration (NASA) said that the Mars Reconnaissance Orbiter (MRO) had returned more than 298 terabits of data as of March 2016 [11]. Also, the NASA expresses with its maximum data rate of 5.2 megabits per second (Mbps), MRO requires 7.5 hours to empty its onboard recorder, and 1.5 hours to send a single HiRISE (High Resolution Imaging science Experiment) image to be processed back on Earth [11]. Image compression is one of the main methods that can reduce the problems based on removing redundant data. The image compression methods have two subcategories of lossless and lossy compression techniques [12, 13]. The differences between these two methods are that the image quality is high in lossless compression but compression ratio is less versus lossy compression [14, 15]. JPEG and JPEG2000 are two main methods which are widely used in different fields [16-18]. The JPEG typically uses the discrete cosine transforms as the main core in image compression. Also, The JPEG2000 is defined by the discrete wavelet transforms in order to reduce the volume of image space. In this work, I introduce a new image compression method based on gradient Haar wavelet [19, 20] which can be used in image compression standards for reducing the problems in human communications. The proposed method will show the effect of sloping of scaling function of Haar wavelet on image compression. The statistical experimental results based on Mean Absolute Error (MAE), Peak Signal to Noise Ratio (PSNR), and Structural SIMilarity index (SSIM) show that the proposed method can improve the image compression standards.

This paper is organized as an overview of related works discussed in section 2. I review the gradient Haar wavelet and then I introduce the preliminary image compression algorithm using gradient Haar wavelet transform in section 3. Then, I introduce a new image compression method for increasing the quality of image compression in

Manuscript Received: March 12, 2020; Revised: March 28, 2020; Accepted: April 3, 2020.
* Y. Sadra, Department of Computer Sciences, Shandiz Institute of Higher Education, Mashhad, Iran - 9184686646.
(email: y.sadra@shandiz.ac.ir)
DOI : 10.17010/ijcs/2020/v5/i2&3/152207

section IV. Next, the statistical experimental results are discussed in section V, and finally in Section VI provides a brief conclusion.

## II. OVERVIEW OF RELATED WORKS

In this section, the brief introductions are given to the JPEG and the JPEG2000 structures.

### *A. JPEG*

The JPEG standard (Joint Photographic Experts Group is one of the joint ISO/CCITT committees that defined the first international image compression standard for still images (grayscale and color) [16]. The JPEG standard includes two basic compression methods (lossy and lossless methods) with various modes of operation that have many applications. The JPEG uses the discrete cosine transforms (DCT) for lossy image compression, although there is a predictive method for lossless image compression (JPEG-LS). The JPEG processing includes block splitting, DCT, quantization, and entropy coding. Each block of image matrix is converted to a representation of the frequency domain based on the two dimensional DCT [21]. The method has high compression ratios and low image quality [22].

### *B. JPEG2000*

The JPEG 2000 compression standard is the development of a new standard for the compression of still images [23]. The JPEG 2000 presents both lossy and lossless image compressions. It proposes higher compression ratios for lossy image compression and also works on image tiles to save memory space. The important part of the JPEG standard is the DCT versus the JPEG 2000 compression standard whose main part is the discrete wavelet transform (DWT), that is a method of multi resolution processing [18, 24-26]. The DWT can obtain several approximations of a function at different levels of resolution which the wavelet function and the scaling function of wavelet are major functions in multi resolution processing [26, 27]. The DWT increases compression efficiency because of good capacity in coupling of the numbers and the ability to restore the numbers. Here, I use Haar wavelet transform as the discrete wavelet transform in JPEG2000. Nowadays, it is proposed as a substitute for the JPEG standard.

In simple terms, the JPEG 2000 processing first divides image into several non-overlapping tiles. Then, it accomplishes the DWT, quantization, and entropy coding on each tile that is similar to JPEG [24]. On the DWT part, the JPEG2000 algorithm uses the two dimensional DWT to decompose the original image into four sub images (LL, LH, HL and HH). The sub images are filtered with low pass (L) and high pass filters (H). The LL has been filtered using low pass filters in horizontal and vertical directions, that is the approximated matrix of original image. The HL has been filtered using high pass filter in the vertical direction and low pass filter in the horizontal direction that is a detailed matrix of original image. The LH has been filtered using low pass filter in the vertical direction and high pass filter in the horizontal direction which is a detailed matrix of the original image. The HH has been filtered using high pass filters in both horizontal and vertical directions which is a detailed matrix of original image [23, 24]. The LL image is quarter of the size of the original image and can be decomposed into four new sub images.

## III. GRADIENT HAAR WAVELET

In this section, I first review gradient Haar wavelet transform and then use it in a preliminary image compression algorithm.

### *A. Gradient Haar Wavelet Transform*

The structure of Haar wavelet is the simplest between wavelets. The property causes it to be used in various sciences. The Haar wavelet was proposed in 1909 by Alfred Haar [28]. The gradient Haar wavelet (GHW) has been introduced in our pervious works [19, 20] which is a Haar wavelet with the sloping scaling function. The gradient Haar wavelet (GHW) can be more efficient than Haar wavelet due to sloping scaling function in signal processing because the main base of the signal processing of a wave based on wavelet is the scaling function. If the scaling function can better illustrate the wave in fewer repetitions, then the signal it is processing has more information of the wave [19, 20]. To describe the gradient Haar wavelet (GHW) first considering scaling function of Haar wavelet that changed as a sloping step function

$$\phi(x) = \begin{cases} \gamma\left(x-\frac{1}{2}\right)+1 & 0 \le x < 1 \\ 0 & otherwise \end{cases} \quad (1)$$

where $\gamma$ is the line slop. Then, the Haar wavelet is the function :

$$\psi(x) = \begin{cases} \left(\frac{\gamma^2}{24}+\frac{\gamma}{24}+1\right)\left(2\gamma x-\frac{\gamma}{2}+1\right) & 0 \le x < \frac{1}{2} \\ -\left(\frac{\gamma^2}{24}-\frac{\gamma}{4}+1\right)\left(2\gamma x-\frac{3\gamma}{2}+1\right) & \frac{1}{2} \le x < 1 \\ 0 & otherwise \end{cases} \quad (2)$$

The other mathematical perspective, the scaling and wavelet functions of the GHW transform are as follows:

$$p_0 = \frac{\gamma^2}{24}-\frac{\gamma}{4}+1\ ,\ p_1 = \frac{\gamma^2}{24}+\frac{\gamma}{4}+1 \quad (3)$$

$$\phi(x) = (\frac{\gamma^2}{24}-\frac{\gamma}{4}+1)\ \phi(2x) + (\frac{\gamma^2}{24}+\frac{\gamma}{4}+1)\ \phi(2x-1)$$

$$\psi(x) = (\frac{\gamma^2}{24}+\frac{\gamma}{4}+1)\,\phi(2x)-(\frac{\gamma^2}{24}-\frac{\gamma}{4}+1)\ \phi(2x-1)$$

where, if the $\gamma$ is zero, the functions are the Haar wavelet functions. The GHW in two dimensions is obtained similar to Haar wavelet. A 4×4 GHW transformation matrix is generated as follows:

$$G_1=\begin{vmatrix} \tilde{p}_0(\gamma) & \tilde{p}_1(\gamma) & 0 & 0 \\ 0 & 0 & \tilde{p}_0(\gamma) & \tilde{p}_1(\gamma) \\ \tilde{p}_1(\gamma) & -\tilde{p}_0(\gamma) & 0 & 0 \\ 0 & 0 & \tilde{p}_1(\gamma) & -\tilde{p}_0(\gamma) \end{vmatrix} \ and$$

$$G_2=\begin{vmatrix} \tilde{p}_0(\gamma) & \tilde{p}_1(\gamma) & 0 & 0 \\ \tilde{p}_1(\gamma) & -\tilde{p}_0(\gamma) & 0 & 0 \\ 0 & 0 & 1 & 0 \\ 0 & 0 & 0 & 1 \end{vmatrix}$$

where, $G_1$ and $G_2$ are first approximation matrix and second approximation matrix, respectively. Then, we have a GHW transformation matrix with variable coefficients

$$G_{4\times4} = G_2G_1 = \begin{vmatrix} (\tilde{p}_0(\gamma))^2 & \tilde{p}_0(\gamma)\tilde{p}_1(\gamma) & \tilde{p}_1(\gamma)\tilde{p}_0(\gamma) & (\tilde{p}_1(\gamma))^2 \\ \tilde{p}_1(\gamma)\tilde{p}_0(\gamma) & (\tilde{p}_1(\gamma))^2 & -(\tilde{p}_0(\gamma))^2 & -\tilde{p}_0(\gamma)\tilde{p}_1(\gamma) \\ \tilde{p}_1(\gamma) & -\tilde{p}_0(\gamma) & 0 & 0 \\ 0 & 0 & \tilde{p}_1(\gamma) & -\tilde{p}_0(\gamma) \end{vmatrix} \quad (4)$$

Where, $\tilde{p}_1(\gamma)$ coefficients $\tilde{p}_1(\gamma) = \frac{p_1(\gamma)}{\sqrt{|p_0(\gamma)|^2+|p_1(\gamma)|^2}}$) are scaling function coefficients [20]. The GHW transformations could have many applications in applied sciences [19, 20].

### B. Preliminary Image Compression Algorithm

In this section, an image compression algorithm based on the GHW will be introduced. In other words, I improve the DWT of JPEG2000 algorithm using GHW transform and to obtain the appropriate parameter ($\gamma$) for GHW transform. We can decompose the original image to four sub images (LL, LH, HL, and HH) that all of them are the homologous approximated-detailed matrices of the original image. First, an original image is considered with $M_m\times_m$ matrix. If G is GHW transformation matrix, matrix E can be the first wavelet decomposition which contains the coefficients matrices LL, LH, HL, and HH of the original image. In order that all of coefficients matrices are the approximated-details coefficients matrices, we should find the appropriate value of line slop '$\gamma$' of GHW if coefficients matrices are defined as follows:

$$\begin{bmatrix} LL \triangleq \begin{bmatrix} \tilde{p}_1^{\,2}x_{2i,2j} + \tilde{p}_1\,\tilde{p}_0(\alpha x_{2i,2j-1} + x_{2i-1,2j}) \\ + \tilde{p}_0^{\,2}x_{2i-1,2j-1} \end{bmatrix}_{1\le i,\ j\le m} \\ LH \triangleq \begin{bmatrix} \tilde{p}_1^{\,2}x_{2i,2j-1} + \tilde{p}_1\,\tilde{p}_0(x_{2i-1,2j-1} - x_{2i,2j}) \\ - \tilde{p}_0^{\,2}x_{2i-1,2j} \end{bmatrix}_{1\le i,\ j\le m} \\ HL \triangleq \begin{bmatrix} \tilde{p}_1^{\,2}x_{2i-1,2j} + \tilde{p}_1\,\tilde{p}_0(x_{2i-1,2j-1} - x_{2i,2j}) \\ - \tilde{p}_0^{\,2}x_{2i,2j-1} \end{bmatrix}_{1\le i,\ j\le m} \\ HH \triangleq \begin{bmatrix} \tilde{p}_1^{\,2}x_{2i-1,2j-1} - \tilde{p}_1\,\tilde{p}_0(x_{2i,2j-1} + x_{2i-1,2j}) \\ + \alpha\tilde{p}_0^{\,2}x_{2i,2j} \end{bmatrix}_{1\le i,\ j\le m} \end{bmatrix} \quad (5)$$

Where, $\alpha$ is a constant value and [] are symbols of matrices in all of the paper. The total coefficients of matrix E are as follows:

$$S = \Sigma^m_{i,j=1}x_{i,j} \quad (6)$$

In result, total coefficients of matrices of sub images are as follows:

$$\begin{bmatrix} SLL = \tilde{p}_1^{\,2}\Sigma^m_{i,j=1}x_{2i,2j} + \\ \tilde{p}_1\,\tilde{p}_0\,\Sigma^m_{i,j=1}(\alpha x_{2i,2j-1} + x_{2i-1,2j}) + \tilde{p}_0^{\,2}\Sigma^m_{i,j=1}x_{2i-1,2j-1} \\ S_{LH} = \tilde{p}_1^{\,2}\Sigma^m_{i,j=1}x_{2i,2j-1} + \\ \tilde{p}_1\,\tilde{p}_0\,\Sigma^m_{i,j=1}(x_{2i-1,2j-1} - x_{2i,2j}) - \tilde{p}_0^{\,2}\,\Sigma^m_{i,j=1}x_{2i-1,2j} \\ S_{HL} = \tilde{p}_1^{\,2}\Sigma^m_{i,j=1}x_{2i-1,2j} + \\ \tilde{p}_1\,\tilde{p}_0\,\Sigma^m_{i,j=1}(x_{2i-1,2j-1} - x_{2i,2j}) - \tilde{p}_0^{\,2}\,\Sigma^m_{i,j=1}x_{2i,2j-1} \\ S_{HH} = \tilde{p}_1^{\,2}\Sigma^m_{i,j=1}x_{2i-1,2j-1} - \\ \tilde{p}_1\,\tilde{p}_0\,\Sigma^m_{i,j=1}(x_{2i,2j-1} + x_{2i-1,2j}) + \alpha\tilde{p}_0^{\,2}\,\Sigma^m_{i,j=1}x_{2i,2j} \end{bmatrix} \quad (7)$$

In the normal mode, total coefficients of matrices of sub images (LL, LH, HL, and HH) are not equal. For example, if we consider the difference between two total coefficients of matrices of sub image matrices LH and HL which is equal to a fixed value *k,*

$$S_{LH} = S_{HL} + K \tag{8}$$

Then,

$$\tilde{p}_1^{\,2} C + \tilde{p}_1 \tilde{p}_0 B - \tilde{p}_0^{\,2} A = \tilde{p}_1^{\,2} A + \tilde{p}_1 \tilde{p}_0 B - \tilde{p}_0^{\,2} C + k \tag{9}$$

where A, B, C and D are as following

$$A = \Sigma_{i,j=1}^{m} x_{2i-1,2j}\,, B = \Sigma_{i,j=1}^{m} (x_{2i-1,2j-1} - x_{2i,2j}),$$
$$C = \Sigma_{i,j=1}^{m} x_{2i,2j-1}.$$

Equation (9) can be summarized as follows

$$\tilde{p}_1^{\,2} + \tilde{p}_0^{\,2} = \tfrac{K}{C-A}. \tag{10}$$

By substituting (3) in (10), we have

$$\gamma = \sqrt{6\,\frac{\sqrt{(C-A)(33(C-A)+8K)}-7(C-A)}{C-A}}$$

If the value of k be equal to zero ($k = 0$), sub images inherit the same amount of original image information, then

$\gamma = \sqrt{6\sqrt{33}-42} = 2.7445626465380280i$. As the value of $\gamma$ shows, sub images with the same amount of original image information occur only in a complex space.

Values of $\tilde{p}_0$ and $\tilde{p}_1$ using $\gamma$ are as following:

$$\begin{cases} \tilde{p}_0 = \dfrac{p_0}{\sqrt{|p_0|^2+|p_1|^2}} = 0.5(1-i) \\ \tilde{p}_1 = \dfrac{p_1}{\sqrt{|p_0|^2+|p_1|^2}} = 0.5(1+i) \end{cases} \tag{11}$$

This property of GHW which the values of $\tilde{p}_0$ and $\tilde{p}_1$ show can have a wide range of numbers depending on the application, it is its superiority relative to Haar wavelet.

Therefore, we can carry out image compression using the values of $\tilde{p}_0$ and $\tilde{p}_1$ and based on GHW transformation, that is,

$$E = G^T MG. \tag{12}$$

To consider $\alpha = -1$ elements of the matrix E are as follows

$$\begin{bmatrix} LL \triangleq \left[\dfrac{x_{2i-1,2j} - x_{2i,2j-1}}{2} - \dfrac{x_{2i-1,2j-1} - x_{2i,2j}}{2} i\right]_{1\le i,\ j\le m} \\ LH \triangleq \left[\dfrac{x_{2i-1,2j-1} - x_{2i,2j}}{2} + \dfrac{x_{2i-1,2j} + x_{2i,2j-1}}{2} i\right]_{1\le i,\ j\le m} \\ HL \triangleq \left[\dfrac{x_{2i-1,2j-1} - x_{2i,2j}}{2} + \dfrac{x_{2i-1,2j} + x_{2i,2j-1}}{2} i\right]_{1\le i,\ j\le m} \\ HH \triangleq \left[-\dfrac{x_{2i-1,2j} + x_{2i,2j-1}}{2} + \dfrac{x_{2i-1,2j-1} + x_{2i,2j}}{2} i\right]_{1\le i,\ j\le m} \end{bmatrix} \tag{13}$$

Where, the coefficients matrix E has complex values. In result, we can obtain modulus of the coefficients matrix E as follows:

$$F_{i,j} = |E_{i,j}| \tag{14}$$

where | ⋮⋮ | is symbol of absolute value. Hence, we have four identical sub images that are the approximated-details coefficients matrices of the original image (fig. 1).

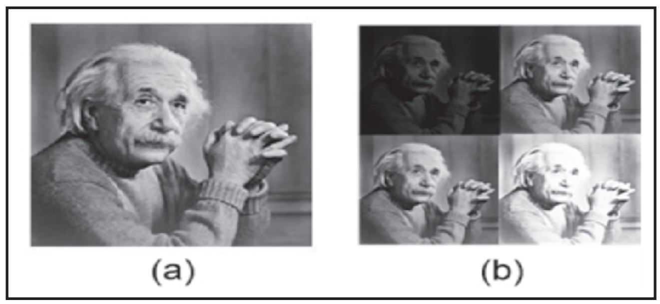

**Fig.1. (a) The Original Image "Einstein"**
**(b) The Modulus of the Coefficients Matrices of 1-level Wavelet Decomposition of the Image using the Gradient Haar Wavelet**

Each sub image can be used for the 2nd level of the wavelet decomposition. Also, they equally inherit the features of the original image.

## IV. THE PROPOSED METHOD

In this section, I propose a new image compression method based on preliminary image compression algorithm that in addition to above advantages has much greater flexibility in data saving. For simplicity in the description of the method, I explain it for a gray image that can easily be generalized to color images. If we look more closely GHW transform, first it divides each matrix of image into blocks of 2×2 and then performs computations on the blocks. Here, we can use the property to develop preliminary image compression algorithm to a new image compression method.

### *A. Compression process*

For simplicity in the description of the algorithm, first, an original image is considered with $M_{m\times m}$ matrix where m is even. The algorithm can be used for $M_{m\times n}$ matrices, where m and n are even and also $m \neq n$ Second, matrix of averages of each block is computed from (13) as follows:

$$S \triangleq [\| \, |Re(HH)| + |Im(HH)\,| \, \|] = \left[\left\| \frac{x_{2i-1,2j-1}+x_{2i,2j}+x_{2i-1,2j}+x_{2i,2j-1}}{4} \right\|\right]_{1\le i,\ j\le m} \quad (15)$$

that $\|\vdots\because\|$ is a round bracket. Then, matrices of differences between elements of the primary diagonal ($N_1$) diagonal and secondary diagonal ($N_2$), and also absolute values $N_1$ and $N_2$ are computed based on Eq.13 as follows :

$$\begin{cases} N_1 \triangleq [-2\ Im(LL)]_{1\le i,\ j\le m} \\ [x_{2i-1,2j-1} - x_{2i,2j}]_{1\le i,\ j\le m} \\ N_2 \triangleq [2\ Re(LL)]_{1\le i,\ j\le m} \\ [x_{2i-1,2j} - x_{2i,2j-1}]_{1\le i,\ j\le m} \\ N_3 \triangleq [|N_1| - |N_2|]_{1\le I,\ j\le m}. \end{cases} \quad (16)$$

To use matrices of differences, we can compute matrix of maximum distances between elements of diagonals as follows:

$$A \triangleq \left[\begin{cases} |N_1|+|N_2|+|N_3|,\ (N_1 \le N_2\ \&\ N_1 \ge 0) \\ \qquad \oplus (N_1 < N_2\ \&\ N_2 \ge 0) \\ -(|N_1|+|N_2|+|N_3|),\ (N_1 \ge N_2\ \&\ N_1 < 0) \\ \qquad \oplus (N_1 < N_2\ \&\ N_2 < 0) \end{cases}\right]_{1\le I,\ j\le m} \quad (17)$$

Where,

$\oplus$ is xor operator and its values can be positive or negative. As a result, we can compute coefficients matrices LH and HL as following

$$\overline{LH} \triangleq \left[\begin{cases} [\lceil S+\lambda\times A \rceil],\ A \ge 0 \\ [\lfloor S+\lambda\times A \rfloor],\ A < 0 \end{cases}\right]_{1\le i,\ j\le m} \quad (18)$$

$$\overline{HL} \triangleq \left[\begin{cases} [\lceil S-\lambda\times A \rceil],\ A \ge 0 \\ [\lfloor S-\lambda\times A \rfloor],\ A < 0 \end{cases}\right]_{1\le i,\ j\le m} \quad (19)$$

Where, $\lambda$ is a balancing coefficient that can be equal to $\frac{1}{8}$ and also $[\lceil\vdots\rceil]$ and $[\lfloor\vdots\rfloor]$ are ceiling brackets and floor brackets, respectively. With this method, the LH and the HL can also save position information of elements of blocks for the diagonal that has the maximum difference between elements (major diagonal). If the $[\overline{lh}_{i,j}]$ is greater than or equal to the $[\overline{hl}_{i,j}]$, it means that the up element of the major diagonal has a larger number. If the $[\overline{lh}_{i,j}]$ is less than the $[\overline{hl}_{i,j}]$, it means that the down element of the major diagonal has a larger number. Consequently, the coefficients matrices LL and HH can be zero

$$\begin{cases} LL \triangleq [0]_{1\le i,\ j\le m} \\ HH \triangleq [0]_{1\le i,\ j\le m}. \end{cases} \quad (20)$$

In order to increase position information of elements of blocks, we use two masks whose sizes are the same the LH and the HL and are defined as follows:

$$B \triangleq \left[\begin{cases} even, & N_1 \ge N_2\ \&\ N_2 \ge 0 \\ Odd, & N_1 \ge N_2\ \&\ N_2 < 0 \\ even, & N_1 < N_2\ \&\ N_1 \ge 0 \\ Odd, & N_1 < N_2\ \&\ N_1 < 0 \end{cases}\right]_{1\le i,\ j\le m} \quad (21)$$

The mask B saves position information of the diagonal that has minimum difference between elements (minor diagonal). If the $[b_{i,j}]$ is even, it means that the up element of the minor diagonal has larger number. If the $[b_{i,j}]$ is odd, it means that the down element of the minor diagonal has a larger number. Here, to note that major and minor diagonals are not mean primary and secondary diagonals.

$$C \triangleq \left[\begin{cases} even,\ (x_{2i-1,2j-1}+x_{2i,2j-1}) \ge (x_{2i,2j}+x_{2i-1,2j}) \\ odd,\ (x_{2i-1,2j-1}+x_{2i,2j-1}) < (x_{2i,2j}+x_{2i-1,2j}) \end{cases}\right]_{1\le i,\ j\le m} \quad (22)$$

The mask C saves position information of columns. If the $[c_{i,j}]$ is even, it means that the left column of the block is greater than or equal to the right column. If the $[c_{i,j}]$ is odd, it means that the left column of the block is less than the right column.

Finally, we filter mask B on the HL and mask C on LH. As a result, we have two details-approximation coefficients matrices that in total are half the size of the matrix of the original image.

$$E \triangleq \begin{bmatrix} 0 & [[\overline{HL}]]_B \\ [[\overline{LH}]]_C & 0 \end{bmatrix} \quad (23)$$

Where, $[[\vdots\because]]$ is symbol of masking. The proposed method has the ability to be combined with other compression methods. An example of a 4×4 matrix is shown as follows :

$$M_{4\times4}=\begin{bmatrix}61&69&79&67\\59&67&81&72\\54&60&74&60\\55&63&61&34\end{bmatrix}.$$

The matrix of averages of each block is as following

$$S_{2\times2}=\begin{bmatrix}64&75\\58&57\end{bmatrix}.$$

Also, matrices of differences between diagonal elements are as follows :

$$N_{1_{2\times2}}=\begin{bmatrix}-6&7\\-9&40\end{bmatrix},\ N_{2_{2\times2}}=\begin{bmatrix}10&-14\\5&-1\end{bmatrix},$$

$$N_{3_{2\times2}}=\begin{bmatrix}-4&-7\\4&39\end{bmatrix}.$$

Therefore, the matrix of maximum distances between diagonal elements is as following

$$A_{2\times2}=\begin{bmatrix}20&-28\\-18&80\end{bmatrix}.$$

In result, coefficients matrices LH and HL with the balancing coefficient $\lambda=\frac{1}{8}$ are as following

$$\overline{LH}_{2\times2}=\begin{bmatrix}67&71\\55&67\end{bmatrix},\ \overline{HL}_{2\times2}=\begin{bmatrix}61&79\\61&47\end{bmatrix}.$$

The mask B and the mask C that save position information of elements of blocks can be obtained as follows

$$B_{2\times2}=\begin{bmatrix}1&0\\0&1\end{bmatrix},C_{2\times2}=\begin{bmatrix}1&0\\1&0\end{bmatrix}$$

where, numbers zero and one are symbol of even and odd, respectively. Finally, to filter mask B on the HL and mask C on the LH, we have compressed matrix E as following :

$$E_{4\times4}=\begin{bmatrix}0&0&61&78\\0&0&60&47\\67&70&0&0\\55&66&0&0\end{bmatrix}.$$

By comparing the matrix E and M, we see that the volume of information of matrix E is half the matrix M. The block diagram of the proposed compressed method is displayed in fig. 2.

### B. Decompression Process

For the decompression process can be almost the same as the compression process but with reverse steps. For more explanation, we describe it as follows :

First, a compressed image (that was compressed by proposed method) is considered with matrix $E_{m\times m}$ that m is even. Then, we can define matrix $\grave{A}$ for each block from $[[\overline{LH}]]_C$ and $[[\overline{HL}]]_B$.

$$\grave{A}\triangleq\begin{bmatrix}\grave{x}_{2i-1,2j-1}&\grave{x}_{2i-1,2j}\\\grave{x}_{2i,2j-1}&\grave{x}_{2i,2j-1}\end{bmatrix}_{1\le i,\ j\le m}\tag{24}$$

and the altered state of matrix $\grave{A}$ can be as follows

$$\grave{A}^T\triangleq\begin{bmatrix}\grave{x}_{2i-1,2j}&\grave{x}_{2i-1,2j-1}\\\grave{x}_{2i,2j}&\grave{x}_{2i,2j-1}\end{bmatrix}_{1\le I,\ j\le m}\tag{25}$$

The elements of the matrix $\grave{A}$ are obtained from comparing the $\overline{LH}$ to the $\overline{HL}$ as follows

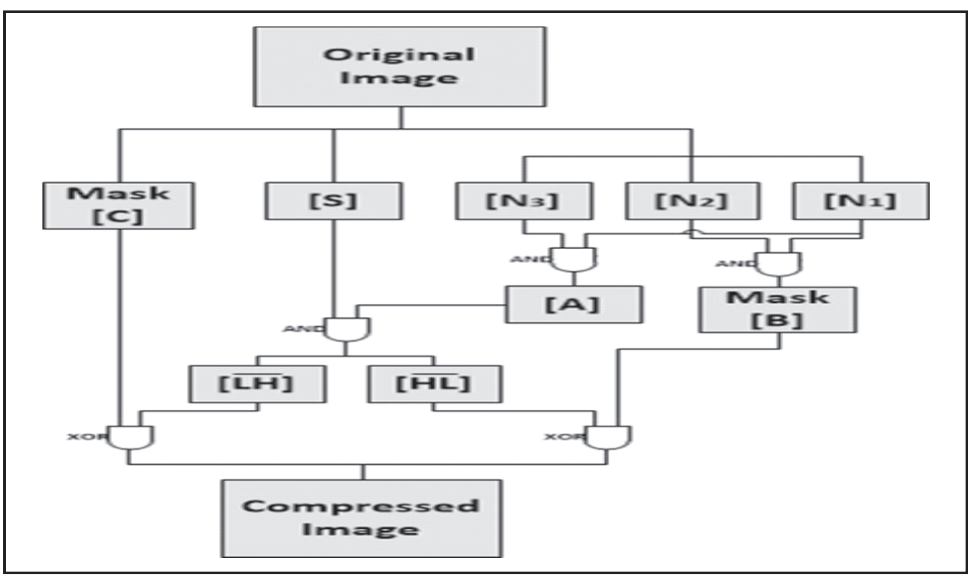


**Fig. 2. The Block Diagram of the Proposed Compressed Method**

$$\grave{x}_{2i-1,2j-1} \triangleq \left[\begin{cases} \dfrac{\overline{lh}_{i,j}+\overline{hl}_{i,j}}{2} + \mu\times|\overline{lh}_{i,j}-\overline{hl}_{i,j}|, \ \overline{lh}_{i,j} \ge \overline{hl}_{i,j} \\ \dfrac{\overline{lh}_{i,j}+\overline{hl}_{i,j}}{2} - \mu\times|\overline{lh}_{i,j}-\overline{hl}_{i,j}|, \ \overline{lh}_{i,j} < \overline{hl}_{i,j} \end{cases}\right]_{1\le i,\ j\le m} \quad (26)$$

$$\grave{x}_{2i-1,2j} \triangleq \left[\begin{cases} \overline{lh}_{i,j}, & (\overline{hl}_{i,j} \ge \overline{lh}_{i,j}\ \&\ \overline{hl}_{i,j}\, be\, odd) \\ & \oplus\ (\overline{hl}_{i,j} < \overline{lh}_{i,j}\ \&\ \overline{hl}_{i,j}\, be\, even) \\ \overline{hl}_{i,j}, & (\overline{hl}_{i,j} < \overline{lh}_{i,j}\ \&\ \overline{hl}_{i,j}\, be\, odd) \\ & \oplus\ (\overline{hl}_{i,j} \ge \overline{lh}_{i,j}\ \&\ \overline{hl}_{i,j}\, be\, even) \end{cases}\right]_{1\le i,\ j\le m} \quad (27)$$

$$\grave{x}_{2i,2j-1} \triangleq \left[\begin{cases} \overline{hl}_{i,j}, & (\overline{hl}_{i,j} \ge \overline{lh}_{i,j}\ \&\ \overline{hl}_{i,j}\, be\, odd) \\ & \oplus\ (\overline{hl}_{i,j} < \overline{lh}_{i,j}\ \&\ \overline{hl}_{i,j}\, be\, even) \\ \overline{lh}_{i,j}, & (\overline{hl}_{i,j} < \overline{lh}_{i,j}\ \&\ \overline{hl}_{i,j}\, be\, odd) \\ & \oplus\ (\overline{hl}_{i,j} \ge \overline{lh}_{i,j}\ \&\ \overline{hl}_{i,j}\, be\, even) \end{cases}\right]_{1\le i,\ j\le m} \quad (28)$$

and also

$$\grave{x}_{2i,2j} \triangleq \left[\begin{cases} \dfrac{\overline{lh}_{i,j}+\overline{hl}_{i,j}}{2} - \mu\times|\overline{lh}_{i,j}-\overline{hl}_{i,j}|, \ \overline{lh}_{i,j} \ge \overline{hl}_{i,j} \\ \dfrac{\overline{lh}_{i,j}+\overline{hl}_{i,j}}{2} + \mu\times|\overline{lh}_{i,j}-\overline{hl}_{i,j}|, \ \overline{lh}_{i,j} < \overline{hl}_{i,j} \end{cases}\right]_{1\le i,\ j\le m} \quad (29)$$

where $\mu$ is a recursive balancing coefficient that is equal to 0.97. We can define matrices $\grave{N}_1$ and $\grave{N}_2$ as follows :

$$\begin{cases} \grave{N}_1 \triangleq [\grave{x}_{2i-1,2j-1} + \grave{x}_{2i,2j-1}]_{1\le i,\ j\le m} \\ \grave{N}_2 \triangleq [\grave{x}_{2i,2j} + \grave{x}_{2i-1,2j}]_{1\le i,\ j\le m} \end{cases} \quad (30)$$

the matrix $\grave{B}$ is obtained from the $\grave{N}_1$, the $\grave{N}_2$ and the $\overline{LH}$ as follows :

$$\grave{B} \triangleq \left[\begin{cases} \grave{A}, & (\grave{n}_{1i,j} < \grave{n}_{2i,j}\ \&\ lh_{i,j}\, be\, odd) \\ & \oplus\ (\grave{n}_{1i,j} \ge \grave{n}_{2i,j}\ \&\ lh_{i,j}\, be\, even) \\ \grave{A}^T, & (\grave{n}_{1i,j} \ge \grave{n}_{2i,j}\ \&\ lh_{i,j}\, be\, odd) \\ & \oplus\ (\grave{n}_{1i,j} \ge \grave{n}_{2i,j}\ \&\ lh_{i,j}\, be\, even) \end{cases}\right]_{1\le i,\ j\le m} \quad (31)$$

As a result, the decompressed matrix $\grave{M}$ is obtained as follows

$$\grave{M} \triangleq [||\grave{B}||]_{1\le i,\ j\le m} \quad (32)$$

$||\vdots\because\vdots||$ is a round bracket. This example can be used to decompress the process as follows :

$$E_{4\times4} = \begin{bmatrix} 0 & 0 & 61 & 78 \\ 0 & 0 & 60 & 47 \\ 67 & 70 & 0 & 0 \\ 55 & 66 & 0 & 0 \end{bmatrix}.$$

The matrix $\grave{A}$ and the altered state of it $\grave{A}^T$ are obtained as follows :

$$\grave{A}_{4\times4} = \begin{bmatrix} 70 & 61 & 66 & 78 \\ 67 & 58 & 70 & 82 \\ 52.5 & 60 & 75.5 & 47 \\ 55 & 62.5 & 66 & 37.5 \end{bmatrix},$$

$$\grave{A}^T_{4\times4} = \begin{bmatrix} 61 & 70 & 78 & 66 \\ 58 & 67 & 82 & 70 \\ 60 & 52.5 & 47 & 75.5 \\ 62.5 & 55 & 37.5 & 66 \end{bmatrix}.$$

Where, the recursive balancing coefficient is $\mu = 0.97$. As a result, the matrix $\grave{B}$ is obtained as follows :

$$\grave{B}_{4\times4} = \begin{bmatrix} 61 & 70 & 78 & 66 \\ 58 & 67 & 82 & 70 \\ 52.5 & 60 & 75.5 & 47 \\ 55 & 62.5 & 66 & 37.5 \end{bmatrix}.$$

Finally, the decompressed matrix $\grave{M}$ is obtained as follows:

$$\grave{M}_{4\times4} = \begin{bmatrix} 61 & 70 & 78 & 66 \\ 58 & 67 & 82 & 70 \\ 53 & 60 & 76 & 47 \\ 55 & 63 & 66 & 38 \end{bmatrix}.$$

A mean absolute error (MAE) between $M_{4\times4}$ and $\grave{M}_{4\times4}$ is equal to 2. Whatever the matrix size is larger, the MAE is close to zero.

Fig. 3 illustrates the steps of proposed method on original images. The block diagram of the proposed decompressed method is displayed in fig. 4.

The proposed method can has more iteration, that is, we can several times iterate the algorithm on sub images. Also, the algorithm can be combined with other coding and algorithms to increase the compression rate.

## V. IMAGE QUALITY MEASURE AND STATISTICAL ANALYSIS

The proposed method is simulated on a moderate system (Intel i3 processor with 4 GB RAM) based on MATLAB™ version 7.10 and is tested on standard 8-bit/pixel grayscale bitmap images with size 512×512 of pixels which have been updated on Google Drive :

(https://drive.google.com/drive/folders/0B7j_o4refVy

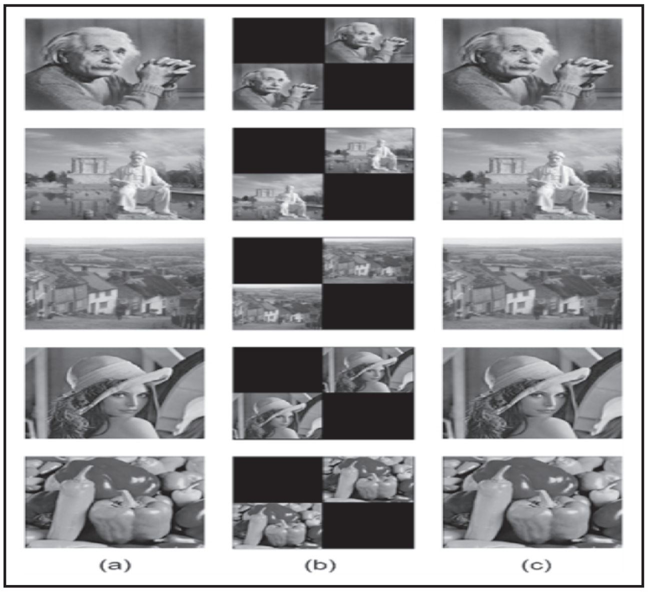


**Fig. 3. (a) The original images ''Einstein, Ferdowsi, Goldhill, Lena, Peppers''. (b) The Details-Approximation Coefficients Matrices of 1-Level Decomposition of the Images Using the Proposed Compressed Method. (c) The Reconstructed Images Using the Proposed Decompressed Method.**

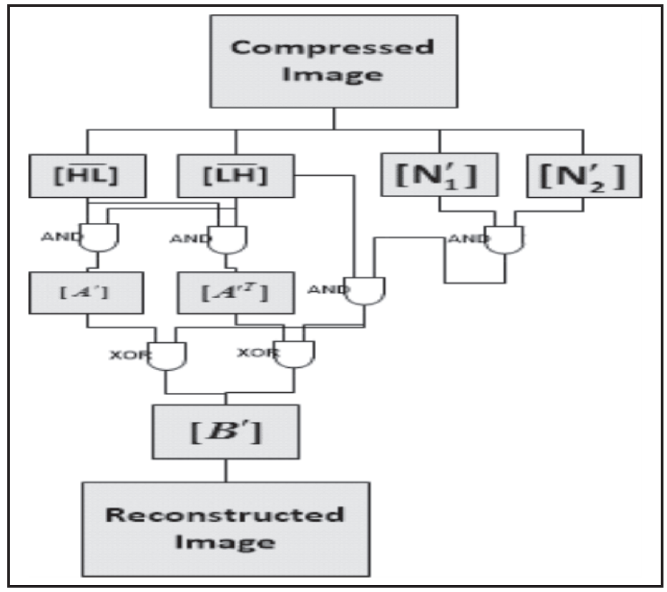


**Fig. 4. The Block Diagram of the Proposed Decompressed Method**

3RG5lZ25veDFmMms). There are many parametric measures to examine the quality of an image such as Compression Ratio (CR), Mean Absolute Error (MAE), Peak Signal to Noise Ratio (PSNR), and Structural SIMilarity index (SSIM). The CR is the ratio of uncompressed size $|M|$of the original image to compressed size $|E|$ of the original image, that is, $CR=\frac{|M|}{|E|}$.

The MAE is defined as follows

$$MAE = \tfrac{1}{m\times n}\Sigma^{m}_{i=1}\Sigma^{m}_{j=1}|M(i,j)-\grave{M}(i,j)| \quad (33)$$

where, the $M(i,j)$ and $\grave{M}(i,j)$ are pixels of the original image and the reconstructed image respectively. If $M(i,j)$ and $\grave{M}(i,j)$ are very close to each other, the MAE can be close to zero. The PSNR is the ratio between the maximum possible power of a signal and the point wise difference between the original image and the reconstructed image which is represented as the following equation :

$$PSNR = 10\log_{10}255^2/\,\mathrm{MSE} \quad (34)$$

that Mean Square Error (MSE) is as

$$MSE = \tfrac{1}{m\times n}\Sigma^{m}_{i=1}\Sigma^{m}_{j=1}(M(i,j)-\grave{M}(i,j))^2 \quad (35)$$

The range of PSNR is between 0 and 100 dB. Good reconstructed images usually have PSNR values more than 30 dB. The SSIM index determines the similarity between original and reconstructed images [29]. Also, the SSIM index can examine the image resolution using a plain reference image. The SSIM index is defined as follows [30]

$$SSIM(m,\grave{m}) = \frac{(2\mu_m\mu_{\grave{m}}+C_1)(2\sigma_{m\grave{m}}+C_2)}{(\mu_m^{\,2}+\mu_{\grave{m}}^{\,2}+C_1)(\sigma_m^{\,2}+\sigma_{\grave{m}}^{\,2}+C_2)} \quad (36)$$

where $\mu_m$, $\mu_{\grave{m}}$, $\sigma_m^{\,2}$, $\sigma_{\grave{m}}^{\,2}$, $\sigma_{m\grave{m}}$ are averages, variances, and covariance of $m$ and $\grave{m}$, respectively. Also, $\{C_i\}_{i=1,2}$ are two variables to stabilize the division with weak denominators which are obtained as $C_i = (k_i L)^2$ with $L$=255, $k_1$=0.01and $k_2$=0.03 [29].

Here, in order to show the abilities of the proposed method, we use proposed method without quantization and entropy coding. Therefore, it has been compared to the original lossy modes of JPEG and JPEG2000 (based on Haar wavelet) methods.

As we know, MAE is a scale-dependent accuracy measure which shows the accuracy of restored values [31]. Tables I, II, and III are presenting the quantitative comparison between JPEG, JPEG2000 (based on 1-level, 2-level, and 3-level decompositions) and proposed method (based on 1-level, 2-level, and 3-level decompositions) using MAE for Compression Ratios of 2, 4, and 8. Results show in compression ratios, that MAE values of proposed method are lower than half of JPEG and JPEG2000 methods.

The PSNR is an approximation to human perception of reconstruction quality [32]. In Tables IV, V, and VI, we see that the PSNR values show the performance of the proposed method transcends JPEG and JPEG2000 methods.

TABLE I.

MAE RESULTS OF RECONSTRUCTED IMAGES FOR CR=2

| Image | JPEG | JPEG2000 | Proposed Method |
|---|---|---|---|
| Einstein | 2.3618 | 2.6810 | 1.2185 |
| Ferdowsi | 2.4801 | 2.3107 | 0.9816 |
| Goldhill | 2.7583 | 2.4829 | 1.0873 |
| Lena | 2.1679 | 2.0683 | 0.8206 |
| Peppers | 2.3180 | 2.1685 | 1.0951 |

TABLE II.

MAE RESULTS OF RECONSTRUCTED IMAGES FOR CR=4

| Image | JPEG | JPEG2000 | Proposed Method |
|---|---|---|---|
| Einstein | 5.2584 | 5.3143 | 2.5615 |
| Ferdowsi | 4.8146 | 4.6285 | 2.0012 |
| Goldhill | 5.3483 | 5.0963 | 2.2361 |
| Lena | 4.3791 | 4.1465 | 1.7983 |
| Peppers | 4.4567 | 4.2624 | 2.2328 |

TABLE III.

MAE RESULTS OF RECONSTRUCTED IMAGES FOR CR=8

| Image | JPEG | JPEG2000 | Proposed Method |
|---|---|---|---|
| Einstein | 9.7849 | 9.8457 | 4.8816 |
| Ferdowsi | 9.3103 | 9.0684 | 4.0864 |
| Goldhill | 9.9576 | 9.5981 | 4.3943 |
| Lena | 8.4180 | 8.1763 | 3.6402 |
| Peppers | 8.9962 | 8.3475 | 4.3726 |

TABLE IV.

PSNR RESULTS OF RECONSTRUCTED IMAGES FOR CR=2

| Image | JPEG | JPEG2000 | Proposed Method |
|---|---|---|---|
| Einstein | 28.3691 | 34.7503 | 41.5819 |
| Ferdowsi | 29.3857 | 35.1387 | 43.1670 |
| Goldhill | 31.3890 | 36.2751 | 44.1538 |
| Lena | 31.7902 | 36.4950 | 44.8604 |
| Peppers | 31.5089 | 35.8265 | 43.5937 |

TABLE V.

PSNR RESULTS OF RECONSTRUCTED IMAGES FOR CR=4

| Image | JPEG | JPEG2000 | Proposed Method |
|---|---|---|---|
| Einstein | 23.1684 | 28.4831 | 35.1356 |
| Ferdowsi | 24.0059 | 29.0500 | 37.2223 |
| Goldhill | 26.2347 | 30.3772 | 38.0521 |
| Lena | 26.5468 | 30.5374 | 38.6114 |
| Peppers | 26.4261 | 29.9899 | 37.4348 |

TABLE VI.

PSNR RESULTS OF RECONSTRUCTED IMAGES FOR CR=8

| Image | JPEG | JPEG2000 | Proposed Method |
|---|---|---|---|
| Einstein | 19.2350 | 28.4831 | 30.1286 |
| Ferdowsi | 20.3191 | 29.0500 | 32.4086 |
| Goldhill | 22.0019 | 30.3772 | 33.2189 |
| Lena | 22.4831 | 30.5374 | 33.5280 |
| Peppers | 22.3890 | 29.9899 | 32.5178 |

TABLE VII.

SSIM RESULTS OF RECONSTRUCTED IMAGES FOR CR=2

| Image | JPEG | JPEG2000 | Proposed Method |
|---|---|---|---|
| Einstein | 0.9553 | 0.9768 | 0.9940 |
| Ferdowsi | 0.9637 | 0.9829 | 0.9961 |
| Goldhill | 0.9675 | 0.9843 | 0.9968 |
| Lena | 0.9701 | 0.9899 | 0.9989 |
| Peppers | 0.9762 | 0.9928 | 0.9997 |

TABLE VIII.

SSIM RESULTS OF RECONSTRUCTED IMAGES FOR CR=4

| Image | JPEG | JPEG2000 | Proposed Method |
|---|---|---|---|
| Einstein | 0.9468 | 0.9674 | 0.9833 |
| Ferdowsi | 0.9542 | 0.9714 | 0.9857 |
| Goldhill | 0.9567 | 0.9736 | 0.9860 |
| Lena | 0.9608 | 0.9792 | 0.9881 |
| Peppers | 0.9673 | 0.9812 | 0.9894 |

The SSIM values of proposed method are compared with the SSIM values of JPEG and JPEG2000 methods in Tables VII, VIII, and IX. The results show that the proposed method improves the image quality of reconstructed images compared with the other two methods.

TABLE IX.

SSIM RESULTS OF RECONSTRUCTED IMAGES FOR CR=8

| Image | JPEG | JPEG2000 | Proposed Method |
|---|---|---|---|
| Einstein | 0.9359 | 0.9561 | 0.9728 |
| Ferdowsi | 0.9430 | 0.9601 | 0.9749 |
| Goldhill | 0.9458 | 0.9620 | 0.9751 |
| Lena | 0.9502 | 0.9689 | 0.9775 |
| Peppers | 0.9569 | 0.9719 | 0.9786 |

TABLE X.

RUNNING TIME RESULTS OF RECONSTRUCTED IMAGES FOR CR=4

| Image | JPEG | JPEG2000 | Proposed Method |
|---|---|---|---|
| Einstein | 1.28 | 0.76 | 0.68 |
| Ferdowsi | 1.32 | 0.71 | 0.61 |
| Goldhill | 1.37 | 0.74 | 0.65 |
| Lena | 1.15 | 0.66 | 0.59 |
| Peppers | 1.27 | 0.69 | 0.63 |

Table X presents the average run time for JPEG, JPEG2000 (based on 2-level decomposition), and proposed method (based on 2-level decomposition) in CR=4. Compared with JPEG, JPEG2000 implemented with MATLAB, the proposed method needs about 0.63s to process one image on an average, which is faster than JPEG2000 (0.71s) and JPEG (1.27s).

In general, the statistical results show that the proposed method is a lossy compression method with high performance. Also, the results show that the proposed method can raise quality of image compression techniques if image compression standards are based on it.

## VI. CONCLUSION

In this paper, I have proposed a new image compression method based on gradient Haar wavelet. The proposed method was using gradient Haar wavelet transform in order to increase image quality of reconstructed image and decrease in size of compressed image simultaneously. Also, the results of the proposed method were compared with JPEG and JPEG2000 (based on Haar wavelet) methods. The statistical results showed that the advantage of the proposed method is higher than that of the other same level methods. Therefore, I propose the proposed method is used in image compression standards.

## REFERENCES

[1] M. N. Do, D. H. Nguyen, H. T. Nguyen,D. Kubacki, and S. J. Patel, "Immersive visual communication," *IEEE Signal Process. Mag.*, vol. *28*, no. *1*, pp. 58-66, 2011. Doi: 10.1109/MSP.2010.939075

[2]F. Yang and S. Wan, "Bitstream-based quality assessment for networked video: A review," *IEEE Commun. Mag.,*, vol. *50*, no. *11*, pp. 203-209, 2012. Doi: 10.1109/MCOM.2012.6353702

[3] A. Borji and L. Itti, "State-of-the-art in visual attention modeling," *IEEE Trans. on Pattern Anal. and Mach. Intell.*, vol. *35*, no. *1*, pp. 185-207, 2013. Doi: 10.1109/TPAMI.2012.89

[4] K. Ma, H. Yeganeh, K. Zeng and Z. Wang, "High dynamic range image compression by optimizing tone mapped image quality index," in *IEEE Trans. on Image Process.*, vol. *24*, no. *10*, pp. 3086-3097, Oct. 2015.

[5] A. Taneja, L. Ballan and M. Pollefeys, "Geometric change detection in urban environments using images," in *IEEE Trans. on Pattern Analysis and Mach. Intell.*, vol. *37*, no. *11*, pp. 2193-2206, 2015. Doi: 10.1109/TPAMI.2015.2404834

[6] H. Nejati, V. Pomponiu, T. T. Do, Y. Zhou, S. Iravani, and N. M. Cheung, "Smartphone and mobile image processing for assisted living: Health-monitoring apps powered by advanced mobile imaging algorithms," in *IEEE Signal Process. Mag.*, vol. *33*, no. *4*, pp. 30-48, July 2016. Doi: 10.1109/MSP.2016.2549996

[7] R. Wang et al., "The MPEG internet video-coding standard [Standards in a Nutshell]," in *IEEE Signal Process. Mag.,* vol. *33*, no. *5*, pp. 164-172, 2016. Doi: https://doi.org/10.1109/MSP.2016.2571440

[8] J. Portilla, V. Strela, M. J. Wainwright, and E. P. Simoncelli, "Image denoising using scale mixtures of Gaussians in the wavelet domain," in *IEEE Trans. on Image Process.*, vol. *12*, no. *11*, pp. 1338-1351, 2003. Doi: 10.1109/TIP.2003.818640

[9] Y. Kwon, K. I. Kim, J. Tompkin, J. H. Kim, and C.

Theobalt, "Efficient learning of image super-resolution and compression artifact removal with semi-local Gaussian processes," in *IEEE Trans. on Pattern Analysis and Mach. Intell.*, vol. *37*, no. *9*, pp. 1792-1805, 2015. Doi: 10.1109/TPAMI.2015.2389797

[10] B. E. Usevitch, "A tutorial on modern lossy wavelet image compression: Foundations of JPEG 2000," *IEEE Signal Process. Mag.*, vol. *18*, no. *5*, pp. 22-35, Sep 2001. Doi: 10.1109/79.952803

[11] J. Zumberge, L. Deutsch and S. Townes, "Deep space communications," in JPL Publication 400-1385. Jet Propulsion Laboratory, California Inst. of Technol. (Pasadena, CA), 2017. [Online]. Available: https://scienceandtechnology.jpl.nasa.gov/research/research-topics-list/communications-computing-software/deep-space-communications

[12] A. M. Rufai, G. Anbarjafari, ands H. Demirel, "Lossy image compression using singular value decomposition and wavelet difference reduction," in *Digital Signal Process.*, vol. *24*, pp. 117-123, 2014. Doi: https://doi.org/10.1016/j.dsp.2013.09.008

[13] N. Goel and S. Gabarda, "Lossy and lossless image compression using Legendre polynomials," in *2016 Conf. on Advances in Signal Process. (CASP)*, Pune, pp. 315-320, 2016. Doi: 10.1109/CASP.2016.7746187

[14] F. Sheng, A. Bilgin, P. J. Sementilli and M. W. Marcelling, "Lossy and lossless image compression using reversible integer wavelet transforms," *Proc. 1998 Int. Conf. on Image Process.* ICIP98 (Cat. No.98CB36269), Chicago, IL, vol *3*., pp. 876-880, 1998. doi: 10.1109/ICIP.1998.727392

[15] C. Lan, J. Xu, W. Zeng and F. Wu, "Compound image compression using lossless and lossy LZMA in HEVC," *2015 IEEE Int. Conf. on Multimedia and Expo (ICME)*, Turin, pp. 1-6, 2015. Doi: 10.1109/ICME.2015.7177430

[16] G. K. Wallace, "The JPEG still picture compression standard," in *IEEE Trans. on Consumer Electronics*, vol. *38*, no. *1*, pp. xviii-xxxiv, Feb 1992. Doi: 10.1109/30.125072

[17] A. Skodras, C. Christopoulos and T. Ebrahimi, "The JPEG 2000 still image compression standard," in *IEEE Signal Process. Mag.*, vol. *18*, no. *5*, pp. 36-58, Sep 2001. Doi: 10.1109/30.125072

[18] M. Rabbani and R. Joshi, "An overview of the JPEG2000 still image compression standard (2002)," *Signal Process.: Image Commun.*, vol. *17*, no. *1*, pp.3-48, 2002. Doi: https://doi.org/10.1007/978-0-387-78414-4_99

[19] S. Ahadpour and Y. Sadra, "Chaotic trigonometric Haar wavelet with focus on image encryption," *J. of Discrete Math. Sciences and Cryptography*, vol. *20*, no. *5*, pp. 1217-1239. 10.1080/09720529.2016.1187958, 2017.

[20] S. Ahadpour, Y. Sadra and M. Sadeghi, "Image encryption based on gradient Haar wavelet and rational order chaotic maps," *Annals. Comput. Sci. Series*, vol. *14*, no. *1*, pp. 59-66, 2016.

[21] N. Ahmed, T. Natarajan and K. R. Rao, "Discrete cosine transform," *IEEE Trans. on Comput.,* vol. *C-23*, no. *1*, pp. 90-93, Jan. 1974. Doi: 10.1109/T-C.1974.223784

[22] J. L. Mitchell and W. B. Pennebaker, "JPEG: Still image data compression standard," *Springer (3rd Ed.)*, 1993.

[23] C. Christopoulos, A. Skodras and T. Ebrahimi, "The JPEG2000 still image coding system: An overview," in *IEEE Trans. on Consumer Electronics*, vol. *46*, no. *4*, pp. 1103-1127, 2000. Doi: 10.1109/30.920468

[24] D. Taubman, "High performance scalable image compression with EBCOT," in *IEEE Trans. on Image Process*., vol. *9*, no. *7*, pp. 1158-1170, 2000. Doi: 10.1109/83.847830

[25] S. G. Mallat, "A theory for multiresolution signal decomposition: The wavelet representation," in *IEEE Trans. on Pattern Analysis and Mach. Intell.*, vol. *11*, no. *7*, pp. 674-693, 1989.

[26] R. C. Gonzalez and R. E. Woods, *Digital image processing*, in John Wiley & Sons (2nd Ed.), Prentice Hall, New Jersey.

[27] T. Acharya and A. K. Ray, *Image process. principles and appl.*, New Jersey: John Wiley & Sons, 2005.

[28] A. Boggess and F. J. Narcowich, *A first course in wavelets with Fourier analysis*, John Wiley & Sons, (2nd Ed.), 2009.

[29] Z. Wang, E. P. Simoncelli and A. C. Bovik, "Multiscale structural similarity for image quality assessment," *The Thrity-Seventh Asilomar Conf. on Signals, Systems & Comput*., vol. *2*, pp. 1398-1402, 2003.

[30] Z. Wang, A. C. Bovik, H. R. Sheikh and E. P. Simoncelli, "Image quality assessment: From error visibility to structural similarity," *IEEE Trans. on Image Process.*, vol. *13*, no. *4*, pp. 1-14, 2004.

[31] R. J. Hyndman and A. B. Koehler, "Another look at measures of forecast accuracy," *Int. J. of Forecasting,* vol. *22*, no. *4*, pp. 679-688, 2006. Doi: https://doi.org/10.1016/j.ijforecast.2006.03.001

[32] Q. Huynh-Thu and M. Ghanbari, "Scope of validity of PSNR in image/video quality assessment," *Electronics Letters*, vol. *44*, no. *13*, pp. 800-801, 2008. Doi; 10.1049/el:20080522

## About the Author

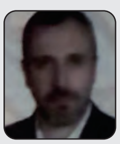

**Yaser Sadra** is Lecturer at Department of Computer Sciences, Shandiz Institute of Higher Education, Mashhad, Iran. He received M.Sc. degree from University of Mohaghegh Ardabili in Iran. His research interests include wavelet, cryptography, image processing, and complex network analysis.